ARCTIC
VOL. 76, NO. 1 (MARCH 2023) P. 1–13
https://doi.org/10.14430/arctic76227

Assessing Ice Island Drift Patterns, Ice Island Grounding Locations, and Gridded Bathymetry Products between Nares Strait and the North Atlantic

Anna Crawford[1] and Derek Mueller[2]

(*Received 24 August 2021; accepted in revised form 12 July 2022*)

ABSTRACT. Large, tabular icebergs known as "ice islands" frequently transit the eastern Canadian Arctic and sub-Arctic after breaking away from ice tongues in northern Greenland. Here, we mine the Canadian Ice Island Drift, Deterioration and Detection (CI2D3) Database to contribute a descriptive assessment of the drift and grounding locations of Petermann ice islands (PII) following calving events at the Petermann Glacier in 2008, 2010, and 2012. We also use the CI2D3 Database to demonstrate how gridded bathymetry products can be improved using observations of ice island grounding and knowledge of ice island thickness. We find that most PII fragments followed a common southbound drift route directed by outflow from the Arctic Ocean and the dominant Baffin and Labrador Currents, which are strongest along the steep continental shelf break. Smaller ice islands were more prone to drift into the deeper waters of central Baffin Bay. As previously noted by northern community members, ice islands were also observed to drift into many adjacent sounds, channels, inlets, and straits. PIIs often grounded on shoals in Kane Basin, to the east of Coburg Island, and along the southeast coast of Baffin Island. Potential inaccuracies in two gridded bathymetry products were located in Jones Sound, near Coburg Island, and along the east coast of Baffin Island. Our approach to identifying these potential inaccuracies is shown to be sensitive to the estimate of ice island keel depth. Overall, this work provides synthesized observations of ice island occurrence and grounding as well as an approach to improving bathymetry products in a resource-rich marine region where traffic and industry operations are increasing.

Key words: ice islands; icebergs; ice hazards; risk assessment; Canadian Arctic; Greenland; Petermann Glacier; Newfoundland and Labrador; bathymetry; currents

RÉSUMÉ. Des icebergs tubulaires de grande taille, appelés « îles de glace » transitent souvent dans l'est de l'Arctique canadien et dans la région subarctique après s'être détachés de langues glaciaires du nord du Groenland. Ici, nous dépouillons la base de données canadienne sur la dérive, la détérioration et la détection des îles de glace (CI2D3) afin d'aboutir à une évaluation descriptive des lieux de dérive et d'échouement des îles de glace de Petermann (PII) à la suite d'événements de vêlage du glacier Petermann survenus en 2008, 2010 et 2012. Nous nous servons également de la base de données CI2D3 pour montrer comment les produits bathymétriques peuvent être améliorés au moyen d'observations de l'échouement des îles de glace et de connaissances sur l'épaisseur des îles de glace. Nous avons constaté que la plupart des fragments de PII suivaient une route de dérive commune vers le sud dirigée par le débit sortant de l'océan Arctique et les courants dominants de Baffin et du Labrador, courants qui sont à leur plus fort le long du rebord abrupt du plateau continental. Les îles de glace plus petites étaient plus susceptibles de dériver dans les eaux plus profondes du centre de la baie de Baffin. Comme des membres de communautés nordiques l'ont déjà fait remarquer, il y a également eu des observations d'îles de glace à la dérive dans de nombreux détroits, traits, chenaux et canaux. Les PII se sont souvent échoués sur les hauts-fonds du bassin Kane, à l'est de l'île Coburg, et le long de la côte sud-est de l'île de Baffin. Les inexactitudes potentielles de deux produits bathymétriques quadrillés se trouvaient dans le détroit de Jones, près de l'île Coburg, et le long de la côte est de l'île de Baffin. Il s'avère que la méthode que nous avons adoptée pour déterminer ces inexactitudes potentielles est sensible à l'estimation de la profondeur des quilles des îles de glace. Dans l'ensemble, cette étude a permis d'obtenir des observations synthétisées de l'occurrence et de l'échouement des îles de glace ainsi qu'une méthode visant à améliorer les produits bathymétriques dans une région marine riche en ressources où la circulation et les activités industrielles sont en voie d'augmentation.

Mots clés: îles de glace; icebergs; dangers liés à la glace; évaluation des risques; Arctique canadien; Groenland; glacier Petermann; Terre-Neuve-et-Labrador; bathymétrie; courants

Traduit pour la revue *Arctic* par Nicole Giguère.

[1] Corresponding author: School of GeoSciences, University of Edinburgh, Drummond St., Edinburgh, EH8 9XP, United Kingdom; anna.crawford@ed.ac.uk
[2] Water and Ice Research Laboratory, Department of Geography and Environmental Studies, B349 Loeb Building, Carleton University, Colonel By Drive, Ottawa, Ontario K1S 5B6, Canada

ᓇᓗᓇᐃᔭᖅᓯᒪᓂᖏᑦ: ᐊᖏᔪᖅ, ᒪᓂᕋᑦᑐᑦ ᐱᖃᓗᔭᐃᑦ ᖃᐅᔨᒪᔭᐅᔪᑦ “ᓯᑯ ᕿᑭᖅᑕᐃᑦ” ᐃᖏᕋᖃᑦᑕᕋᔪᑦᑐᑦ ᑲᓇᑖᖓᓂ ᑲᓇᑕᒥ ᒋᑦ ᓯᑰᑉ ᐃᓱᖏᓐᓂ ᐅᐊᓐᓇᖓᓂ ᐊᑯᑭᑦᑐᑦ. ᐅᕙᓂ, ᓂᓪᓚᓐᓂᐊᕐᕕᒋᕙᑦᑕᕗᑦ ᑲᓇᑕᓯ ᓯᑯ ᕿᑭᖅᑕᐃᑦ ᐃᖏᕋᔪᑦ, ᓄᖑᑎᖅᐸᓪᓚᐊᓂᖏᓐᓄᑦ ᐊᒻᒪ ᖃᐅᔨᔭᐅᓂᖏᓐᓄᑦ (CI2D3) ᑐᑭᓯᒋᐊᕈᑎᑦ ᐃᑲᔪᕐᓂᖃᕐᓗᑎ ᓇᓗᓇᐃᔭᖅᓯᒪᔪᓂᑦ ᖃᐅᔨᓴᓂᕐᒥᑦ ᐃᖏᕋᓂᖏᓐᓄ ᐊᒻᒪ ᐃᖅᑲᖓᓄᑦ ᐊᑦᑐᕐᓂᖏᓐᓄᑦ ᓇᒦᓐᓂᖏᑦ Petermann ᓯᑯ ᕿᑭᖅᑕᐃᑦ (PII) ᓯᕐᑰᓗᓚᐅᖅᑎᓪᓗᒋᑦᐅᕙᓂ Petermann ᐊᐅᔨᐃᑦᑐᖅ 2008, 2010 ᐊᒻᒪ 2012. ᐊᑐᓚᐅᕐᒥᔭᕗᑦᑕᐅᖅ CI2D3 ᑐᑭᓯᒋᐊᕈᑏ% ᑕᑯᔅᓴᐅᑎᑦᑎᓗᑎ ᖃᓄᖅ ᐃᖃᖓ ᐱᓚᓗᔭᕐᓄ ᐊᑦᑕᐅᖅᓯᒪᓂᖏᓐᓄᑦ ᐱᐅᓯᑎᒋᐊᖅᑕᐅᔪᓐᓇᕐᒪᖓᑦ ᐊᑐᕐᓗᑎ ᑕᑯᓐᓇᖅᑕᐅᔪᓂᑦ ᓯᕐᑯᓂᑦ ᕿᑭᖅᑕᓂᑦ ᐃᖅᑲᖓᓄᑦ ᐊᑦᑐᑎᓪᓗᒋᑦ ᐊᒻᒪ ᖃᐅᔨᒪᔭᐅᓂᖓ ᓯᑯ ᕿᑭᖅᑕᖅ ᐃᔾᔪᓂᖓ. ᖃᐅᔨᓚᐅᖅᑕᕗᑦ ᐅᒥᒫᓂᖅᓴᐃᑦ PII ᓯᕐᑯᓪᓗᖅᓯᒪᔪᑦ ᑕᒪᐅᓇᔅᓴᐅᓐᓇᖅ ᓂᒋᕐᔫᖅᐸᓚᐅᖅᑐᑦ ᑐᕌᖅᑐᑦ ᐊᓂᕙᓪᓕᐊᓂᖓᓄᑦ ᐃᖏᕋᓂᖓ ᐅᑭᐅᑕᖅᑐᒥ ᐃᒪᖓᓂ ᐊᒻᒪ ᐱᑕᖃᕐᓂᖓ ᕿᑭᖅᑖᓗᒻᒥ ᐊᒻᒪ ᓯᑉᐳᐊᒥ ᐃᖏᕋᓂᖏᑦ, ᑖᒃᑯᐊ ᐃᖏᕋᓂᐅᔪᑦ ᓴᖏᓯᖑᓪᓗᑎ ᐊᒨᐊᐸᓪᓕᐊᔪᓄᑦ ᓯᑯᖓᓂ ᐄᔭᖅᑐᑎ. ᒥᑭᔪᑕᐅᓂᖅᓴᐃᑦ ᓯᑯᐃᑦ ᕿᑭᖅᑕᐃᑦ ᐃᑎᔪᓃᖃᑦᑕᓂᖅᓴᐅᓛᑦ ᕿᑎᐊᓂ ᓴᓐᓂᕈᑎᐅᐸ ᐃᒪᖓᓂ. ᓇᓗᓇᐃᖅᑕᐅᖅᑲᐅᔪᖅ ᐅᑭᐅᑕᖅᑐᒥ ᓄᓇᓕᒻᒥᐅᑕᓄᑦ, ᓯᑯᐃᑦ ᕿᑭᖅᑕᐃᑦ ᑕᑯᔭᐅᖃᑦᑕᖅᑐᑎᑦ ᖃᓂᒋᔭᖏᓐᓄᑦ ᐃᒪᖏᓐᓃᖃᖅᑐᑎᑦ, ᐃᑭᕋᓴᐃᑦ, ᖃᖏᖅᑐᓂᑦ ᐊᒻᒪ ᐊᖅᑯᑎᓄᑦ. PII ᐃᖅᑲᖓᓄᑦ ᐊᑦᑐᕋᔪᑦᑐᑦ ᐃᒃᑲᑦᑐᓂᑦ ᐱᓪᓚᕆᐊᔭᔪᐊᖅ ᐃᒪᕐᑯᑖᓂ, ᑲᓇᓐᓇᖓᓄᑦ ᖁᕐᕕᒃ, ᐊᒻᒪ ᑭᓪᓕᖓᒍᑦ ᓂᒋᖓᑕ ᑲᓇᓐᓇᒍ ᕿᑭᖅᑖᓗᒥ. ᐱᑕᖃᕈᓐᓇᕐᓂᖓ ᐱᑎᐊᖅᓯᒪᖏᑦᑐᑦ ᒪᕐᕈᓐᓂᒃ ᐃᖅᑲᖓᓅᖅᑐᓂᑦ ᐅᕙᓃᓚᐅᖅᑐᑦ Jones Sound, ᖃᓂᒋᔭᖓᓂ ᖁᕐᕕᒃ, ᐊᒻᒪ ᑭᓪᓕᖓᒍᑦ ᑲᓇᓐᓇᖓᒍ ᕿᑭᖅᑖᓗᒃ. ᖃᐅᔨᓴᕐᓂᕆᓂᐊᖅᑕᕗᑦ ᓇᓗᓇᐃᕐᓗᒋᑦ ᑖᒃᑯᐊ ᐱᑕᖃᕈᓐᓇᖅᑐᑦ ᐱᑎᐊᖅᓯᒪᖏᑦᑐᑦ ᑕᑯᔅᓴᐅᑎᑕᐅᓯᒪᔪᑦ ᒥᒃᓴᐅᓴᑎᐊᖅᑕᐅᓯᒪᓇᑎ ᓯᑯᐃᑦ ᕿᑭᖅᑕᐃᑦ ᐃᓱᐊᓈᓐᓂᖅᐸ̇ᖅ ᐃᑎᓂᖓᓄᑦ. ᐊᑕᖏᖅᑐᒍ, ᑖᓐᓇ ᐱᑕᖃᖅᑎᑦᑎᔪᖅ ᓴᓇᔭᐅᓯᒪᔪᓂᑦ ᑕᑯᔭᐅᓂᖏᓐᓄᑦ ᓯᑯᐃᑦ ᕿᑭᖅᑕᐃᑦ ᓴᖅᑭᖃᑦᑕᕐᓂᖏᑦ ᐊᒻᒪ ᐃᖅᑲᖓᓅᖃᑦᑕᕐᓂᖏᑦ ᐊᒻᒪᓗᑦᑕᐅᖅ ᐊᑐᖅᑕᐅᓂᖓ ᐱᐅᓯᑎᒋᐊᖅᑕᐅᓂᖓ ᐃᖅᑲᖓᓅᓂᖓᖅᑐᓂᑦ ᓄᓇᒦᖓᖅᑐᓂᑦ ᐱᑕᖃᑎᐊᖅᑐᓂᑦ ᐃᒪᖓᓂ ᐊᕕᑦᑐᖅᓯᒪᔪᒥᑦ ᐊᒻᒪ ᐱᓕᕆᓂᕐᒧᑦ ᐊᐅᓚᓂᖏᑦ ᖁᕝᕙᐸᓪᓕᐊᓕᖅᑐᑎᑦ.

ᐅᖃᐅᓯᖏᓪᓗᐊᑕᐃᑦ: ᓯᑯᐃᑦ ᕿᑭᖅᑕᐃᑦ; ᐱᖃᓗᔭᐃᑦ; ᓯᑯᐃᑦ ᐊᑦᑕᓇᕈᑎᐅᔪᓐᓇᖅᑐᑦ; ᐊᑦᑕᓇᕈᑎᐅᔪᓐᓇᖅᑐᓂ ᖃᐅᔨᓴᕐᓂᖅ; ᑲᓇᑕᒥ ᐅᑭᐅᑕᖅᑐᖓ; ᐊᑯᑭᑦᑐᑦ; Petermann ᐊᐅᔨᐃᑦᑐᖅ; ᓂᐅᐸᐅᓐᓀᓐ ᐊᒻᒪ ᓛᐸᑐᐊ; ᐃᑎᓂᖓᓂ ᖃᐅᔨᓴᕐᓂᖅ; ᐃᖏᕋᓂᐅᔪᑦ.

INTRODUCTION

Ice shelves and ice tongues, which extend from glaciers or are affixed to land, can calve large, tabular icebergs that are referred to as "ice islands" in the Arctic (Dowdeswell and Jeffries, 2017; Crawford et al., 2018a). A nascent ice island with a surface area of ~180 km^2 currently sits downstream of a rift that nearly transects the Petermann Glacier (PG) ice tongue in northwest Greenland. When this calving occurs it will follow three large PG calving events that occurred between 2008 and 2012. The 2008 Petermann Ice Island (PII-2008) was the smallest with a surface area of 30 km^2; it remained relatively intact as it followed a drift trajectory south through the eastern Canadian Arctic (Peterson et al., 2009; Crawford et al., 2018a, b). The larger PII-2010 (297 km^2) and PII-2012 (137 km^2) also followed this general southbound trajectory, which is directed by the outflow from the Arctic Ocean and the dominant Baffin and Labrador Currents that are concentrated along the continental shelf break (Fissel et al., 1982; Newell, 1993; Tang et al., 2004; Han et al., 2008; Marson et al., 2018). However, the fracturing of the 2010 and 2012 PIIs dispersed hundreds of ice islands and smaller fragments throughout the waters of eastern Canada and western Greenland (Crawford et al., 2018a).

Through their progressive drift and deterioration, ice islands serve as vectors of freshwater and nutrients from the Greenland and Antarctic ice sheets (Smith et al., 2013; Merino et al., 2016; Crawford et al., 2018b). Nunavummiut use *piqalujat* (icebergs) as a source of freshwater, and some have noted an abundance of wildlife in their wake (NIRB, 2019). Ice islands, as well as the icebergs, bergy bits, and growlers that are generated through their ongoing deterioration, are also potential hazards to vessels and oil and gas infrastructure (Hill, 2006; Peterson, 2011; Mueller et al., 2013; Fuglem and Jordaan, 2017). Ice shelves and floating ice tongues in northwest Greenland are likely to continue to calve ice islands as part of natural cycling or in response to climate warming, while the Arctic marine environment is anticipated to become increasingly active (Smith and Stephenson, 2013; Meier et al., 2014; Hill et al., 2017). It is therefore important to know where these ice islands commonly drift and ground. However, there is currently a dearth of easily accessible, synthesized observations of regional ice island occurrence for consideration during policy development. As such, the Nunavut Impact Review Board recommended baseline research into "iceberg presence and distribution" in the Strategic Environmental Assessment in Baffin Bay & Davis Strait (NIRB, 2019:124). In response to this recommendation, we assess the contents of the Canadian Ice Island Drift, Deterioration and Detection (CI2D3) Database (Crawford et al., 2018a; Desjardins et al., 2018) to provide a simple, descriptive assessment of PII drift and grounding locations in relation to the regional bathymetry, which subsequently influences ocean currents and iceberg drift trajectories (Gille et al., 2004; Tang et al., 2004; Crocker et al., 2013). We also demonstrate an approach by which gridded bathymetry products can be improved by comparing seafloor heights with conservatively deep estimates of ice island keel depths.

METHODS

The CI2D3 Database

The CI2D3 Database is available from the Polar Data Catalogue (Desjardins et al., 2018; https://www.polardata.ca/pdcsearch/?doi_id=12678) and contains locational and morphological data for more than 25,000 ice islands that originated from the Petermann, Ryder, Steensby,

and C.H. Osterfeld ice shelves and floating ice tongues in northwest Greenland. The ice islands were manually tracked between August 2008 and December 2013 through the analysis of tens of thousands of images acquired by synthetic aperture radar (SAR) sensors primarily on the Canadian Space Agency's RADARSAT-1 and -2 satellites. The database includes a georeferenced polygon geometry field that represents an ice island's location and surface area, and the lineage of ice islands is captured with a system of unique identifiers. The ice islands were tracked until they deteriorated below 0.25 km^2 in surface area; the database creators endeavoured to obtain, at a minimum, observations of each tracked ice island every two weeks. If repeat observations of an ice island indicated that it had not substantially moved, the ice island's status was assigned as "grounded" as opposed to "trapped" (in sea ice) or "drifting." Database creators logged if there was uncertainty in this assignment; in this study, we only use observations for which the creators were confident in an ice island's grounded status. This certainty was gained by considering sea ice conditions, georeferencing errors in the analysed satellite imagery, and evidence of grounding such as repeated observations of an ice island in the same location and disturbance of pack ice as it was deflected around static ice islands. Such disturbance is identified by open water areas or "wakes" downstream of grounded ice islands (Viehoff and Li, 1995; Luckman et al., 2010). We note that grounded ice islands can move slowly over time as they gouge (scour) the seafloor (Croasdale et al., 2001; Dowdeswell and Bamber, 2007) and often rotate around their grounding point (e.g., Stern et al., 2015).

Here we analyse the CI2D3 Database records associated with observations of ice islands derived from the 2008 (332 records), 2010 (9658 records), and 2012 (7263 records) PG calving events. These records make up 68% of the observations included in the CI2D3 Database. Three data subsets, one for each of the above calving events, were generated through a database query. The calving-event subsets were filtered to include only the first observation of an ice island per two-week time period. This filtering removed sampling bias, as many ice islands were tracked at a greater frequency than the minimum two-week repeat-observation period. Ice islands were also binned into size classes (< 1 km^2, 1 – 10 km^2, 10 – 20 km^2, 20 – 30 km^2, 30 – 40 km^2, 40 – 50 km^2, > 50 km^2) for an assessment of ice island size and observation over varying bathymetry. To investigate grounding locations, the data subsets were filtered to only include the first observation of a grounded ice island. The density of groundings was assessed over a 100 × 100 km grid generated through the functionality of the ggplot2 R package (Wickham et al., 2020).

Bathymetry Products

Bathymetry associated with each ice island location was extracted from two gridded bathymetry products—the National Ocean and Atmospheric Administration ETOPO1 Global Relief Model (Amante and Eakins, 2009; NOAA National Geophysical Data Center, 2009) and the International Bathymetric Chart of the Arctic Ocean (IBCAO v4; Jakobsson et al., 2020). ETOPO1 is gridded at a resolution of 1 arc-minute (1 arc-minute equates to 0.3 km at 80° N and 1.2 km^2 at 50° N) and is global in extent. IBCAO v4 has a resolution of 200 × 200 m and is only available at latitudes above 64° N, therefore only ETOPO1 was used for the assessment of ice island drift trajectories and locations. IBCAO is accompanied by two raster files that provide information on the type and source of data used to derive the bathymetry values for each grid cell. For example, observations from the Canadian Hydrographic Service non-navigational bathymetric data at a resolution of 100 m (NONNA-100) are included, as are multibeam sonar surveys from the CCGS *Amundsen* (up until 2013) and other sources of data. It is therefore possible to assess where the IBCAO grid is supported by observations and where it is extensively interpolated.

Using Ice Island Observations to Improve Gridded Bathymetry Products

We demonstrate an approach to improve gridded bathymetry products using conservatively deep estimates of ice island keel depths (K_d). The approach is illustrated conceptually and with example values in Figure 1. The central concept of this approach is that the shallowest point of the seafloor under a grounded ice island (B_{shall}) cannot be deeper than K_d, otherwise the ice island could not be grounded. In these cases, there would be a positive apparent clearance (i.e., K_d shallower than B_{shall}). To use this approach, one needs observations of ice island groundings and knowledge of the thickness of the grounded ice islands. We demonstrate the approach by flagging potentially inaccurate bathymetric values in the IBCAO and ETOPO1 products using observations of ice island groundings recorded in the CI2D3 Database.

No groundings were recorded after the 2008 PII calving event. K_d values were computed using the thickness calculated from altimetry profiles of the 2010 and 2012 PIIs before they calved from the Petermann Glacier (Münchow et al., 2014). These maximum thickness values were 108 and 228 m, respectively (A. Münchow, pers. comm. 2022). To ensure that K_d is a conservative estimate, we increased these maximum thickness values by 25% and converted them to a maximum iceberg keel depth assuming hydrostatic equilibrium, a pure ice density of 917 kg m^{-3} (Münchow et al., 2014), and seawater density of 1025 kg m^{-3}. This calculation yielded respective K_d values for the 2010 and 2012 PIIs of 121.8 m and 255.0 m.

We used all polygons of an ice island over the time it was grounded at a position for at least two consecutive observations. We then compared K_d against B_{shall}, the latter being the shallowest bathymetry value associated with all pixels that fell under an ice island polygon. All polygons in the CI2D3 Database are associated with

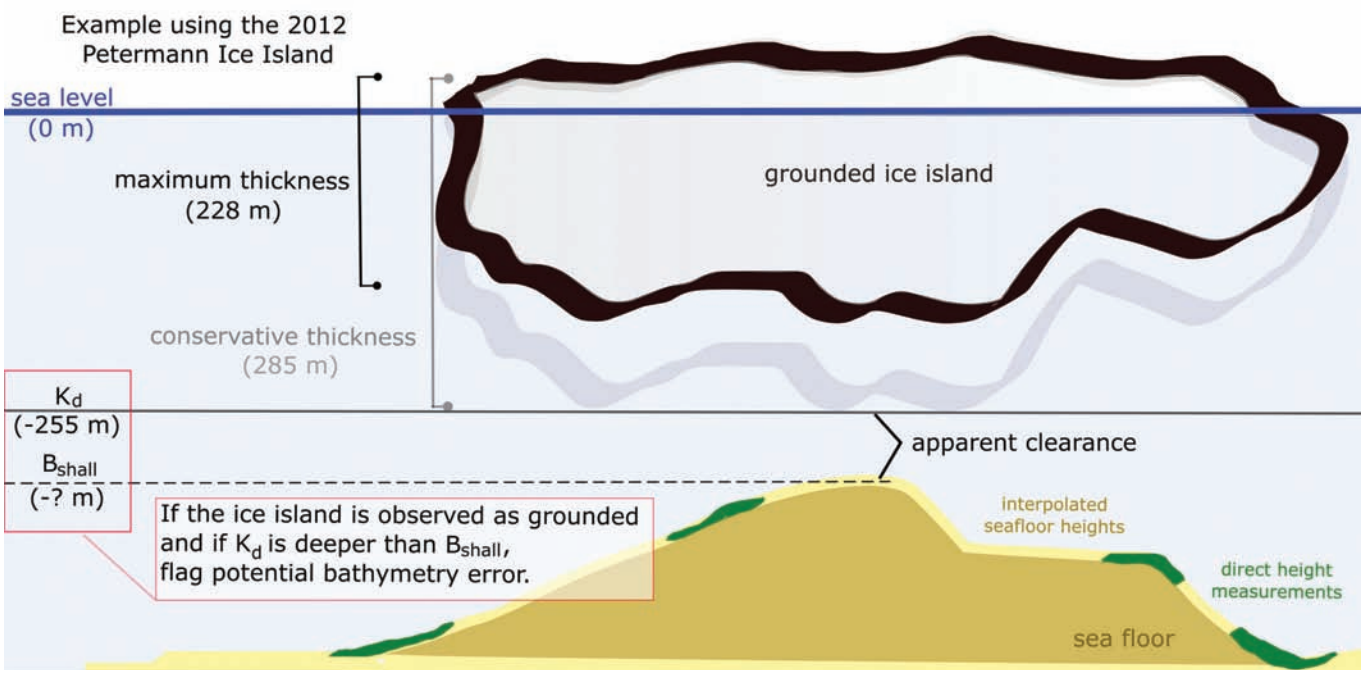

FIG. 1. A conceptual example of how ice island keel depths can be utilised to flag potentially inaccurate bathymetry. K_d is the maximum keel depth estimated for an ice island. B_{shall} is the shallowest bathymetry value associated with the pixels of a gridded product that fall under a grounded ice island polygon. The IBCAO gridded bathymetry product provides the data type of the seafloor height reported for each grid pixel. This study groups these data types into two categories: reliable (derived from direct measurements or pregridded data) and unreliable (interpolated seafloor heights).

a georeferencing error (coded as 0 – 100, 100 – 200, 200 – 400 or > 400 m), which represents potential misalignment in a SAR image's georeferencing. The polygons of the grounded ice islands assessed here were buffered by the maximum georeferencing error before extracting the depths of all coincident IBCAO and ETOPO1 pixels. Ice islands associated with a georeferencing error greater than 400 m were removed from the analysis. We flagged locations in the bathymetry products where there was a positive value in apparent clearance for one or more of the repeat observations associated with the grounding events. This situation suggests that the corresponding bathymetric data are too deep at this location, assuming the ice island keel depth is not deeper than our conservative K_d value.

The IBCAO product provides additional information regarding the type of data associated with each pixel. With this information, we report if the identified locations in the IBCAO product are associated with grid cells with a Type Identifier (TID) that corresponds with "direct" measurements (e.g., soundings, or sonar and seismic surveys; TID between 10 and 17) as opposed to grid interpolation (TID between 40 and 45) and "unknown" sources (TID between 70 and 72). We found that pixels with TID = 70 (pre-generated grid) coincided with the U.S. National Centers for Environmental Information Multibeam Mosaic (https://www.ncei.noaa.gov/maps/bathymetry/). This mosaic includes soundings by the CCGS *Amundsen* (up until 2013) and NONNA-100 (https://data.chs-shc.ca/map). In this way, we classified IBCAO grid cells as being based on observational data (TID between 10 and 17, or 70) or derived through interpolation (TID between 40 and 45). We classify these as "reliable" and "unreliable" data sources, respectively. We report the number of ice island polygons that had a positive apparent clearance while the ice island was grounded, as well as the data class that corresponds to the shallowest ^{B}shall value associated with the flagged polygons of a given grounding event.

The IBCAO v4 product is more recent, includes more observations, and is at a higher resolution than the ETOPO1 data. As a test of our method, we evaluate the hypothesis that locations flagged as potentially inaccurate in the ETOPO1 product (apparent clearance > 0) are not flagged or at least have a reduced clearance in the IBCAO product, in particular if the underlying data are reliable. We do this by comparing flagged groundings in each data set and interpret the results in the context of the IBCAO data type field.

RESULTS

Drift and Bathymetry

The location of ice island descendants of the three major PG calving events are shown in Figure 2 against the bathymetry of the region (derived from ETOPO1). In general, the ice islands followed the typical drift trajectory of ice islands originating in northwest Greenland: south through Nares Strait and Baffin Bay, into the Labrador Sea, and generally hugging the eastern coastlines of Ellesmere, Devon, and Baffin Islands. Those ice islands that made it farther south continued to drift along the continental shelf

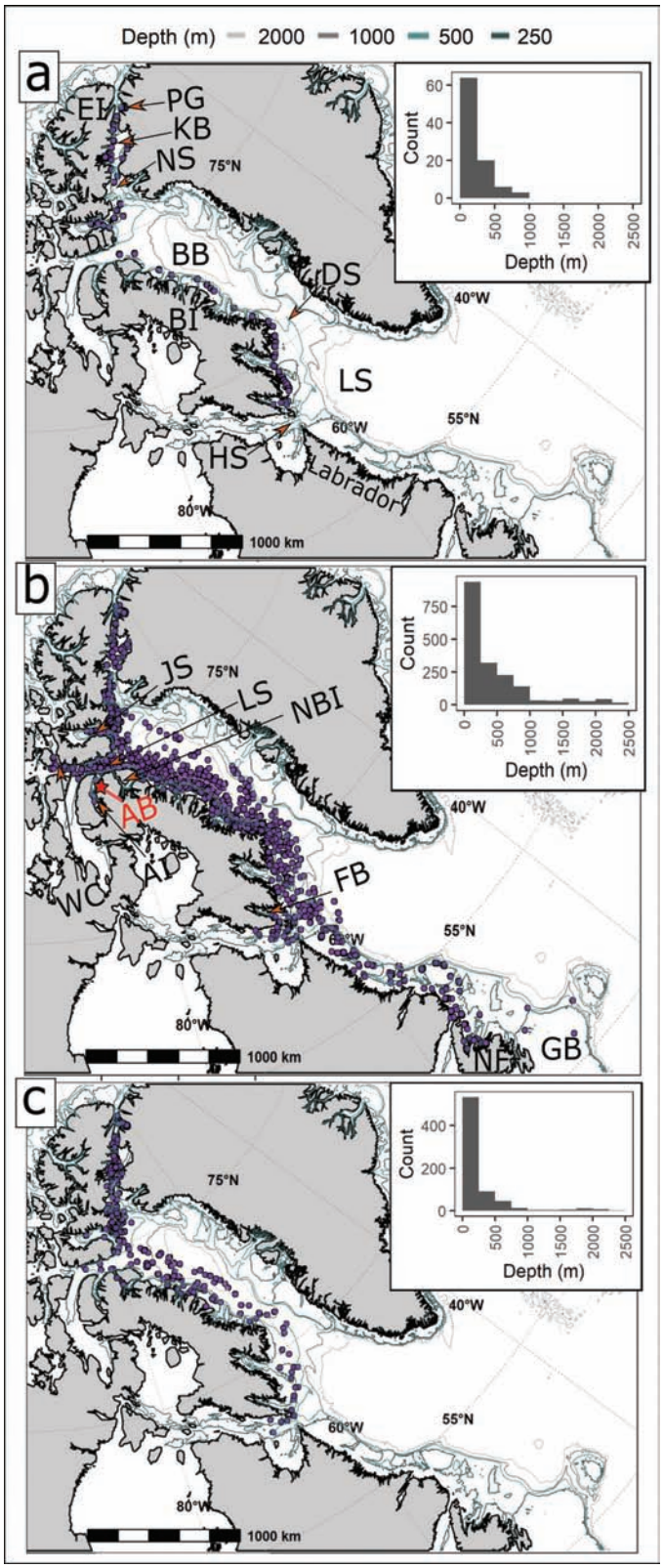

FIG. 2. CI2D3 Database ice island records, filtered on a two-week observation interval, associated with the (a) 2008, (b) 2010, and (c) 2012 Petermann Glacier calving events. Locations of interest: (a) EI = Ellesmere Island, PG = Petermann Glacier, KB = Kane Basin, NS = Nares Strait, BB = Baffin Bay, BI = Baffin Island, DS = Davis Strait, LS = Labrador Sea, HS = Hudson Strait; (b) JS = Jones Sound, LS = Lancaster Sound, WC = Wellington Channel, AI = Admiralty Inlet, AB = Hamlet of Arctic Bay, NBI = Navy Board Inlet, FB = Frobisher Bay, NF = Newfoundland, GB = Grand Banks.

of Labrador and Newfoundland (Fig. 2b). Animations of ice island drift following the 2008, 2010, and 2012 PG calving events are available at https://tinyurl.com/5dz9dkbw.

The 2008 PII remained largely intact during its 13-month existence from July 2008 to August 2009. The main ice island tracked close to eastern Canada as it drifted through Nares Strait, though fragments also followed the 250 m isobath into western Kane Basin and detoured into Jones Sound farther south. This meandering path followed the northern edge of the shelf break before crossing the relatively deep (~880 m) basin of Jones Sound. After exiting Nares Strait, the largest ice island followed the Baffin Island coastline before reaching the mouth of Frobisher Bay. It then fractured into numerous small fragments that quickly fell below the size threshold for inclusion in the CI2D3 Database, though some fragments were observed to drift into Frobisher Bay before tracking ceased (Crawford et al., 2018a, b). Of the 61 ice island observations associated with the 2008 calving event south of Nares Strait, 72% were in water depths less than 250 m.

Similarly, ice islands that originated from the 2010 and 2012 calving events tracked to the west in Nares Strait as they began their southbound transit. Ice islands were also observed in western Kane Basin and Jones Sound. However, successive fracturing multiplied the number of ice islands that transited through Baffin Bay and into more southern waters. Thirty-seven of these ice islands entered the deep (> 700 m) mouth of Lancaster Sound; ice islands originating from the 2010 calving drifted ~350 km west into the sound and looped into Wellington Channel (~150 to 200 m depth). South of Lancaster Sound, ice islands were also observed in Admiralty and Navy Board Inlets following the 2010 and 2012 PG calving events, respectively. Both inlets are relatively deep, with water depths near Ikpiarjuk (the Hamlet of Arctic Bay) on the coast of Admiralty Inlet reaching ~700 m.

The histograms in Figure 2 show that the majority of ice islands were observed in shallower waters (< 500 m depth). However, as shown Figure 2b and c, numerous ice islands associated with the 2010 and 2012 calving events drifted to the centre and eastern regions of Baffin Bay where ice islands were observed in water depths of nearly 2500 m. Panels a – c of Figure 3 show that ice islands in waters of these depths were consistently those of the smallest size classes (0.25 – 1 km^2 and 1 – 10 km^2).

The eastern limit that ice islands reached in Baffin Bay corresponded with the 500 m isobath adjacent to the west coast of southern Greenland. A small number of ice islands were redirected by the northerly Greenland Current, though these ice islands fell below the size threshold for recording in the CI2D3 Database before their final trajectory could be determined. Ice islands that strayed from the eastern coastline of Baffin Island were observed to retrack west to waters under 500 m in depth after funnelling through Davis Strait. The first ice islands that originated from the 2010 PII to reach this location did so seven months after the PG calving event. These ice islands continued south

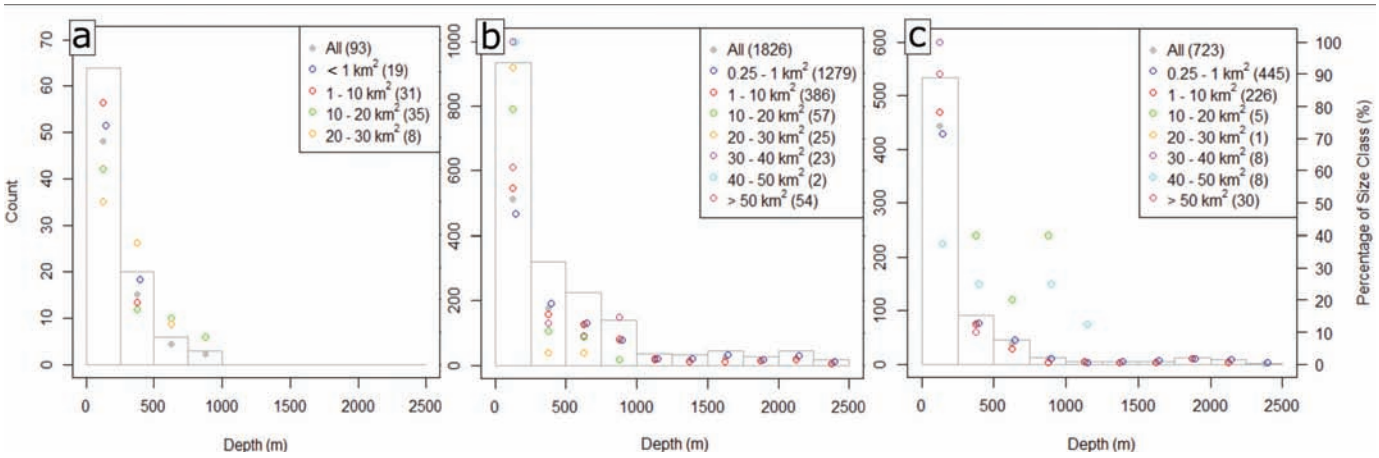

FIG. 3. Observation count of ice islands per 250 m water column depth bin (histograms) and percentage of ice island size class observations per depth bin (points, right-hand y-axis) associated with the (a) 2008, (b) 2010, and (c) 2012 Petermann Glacier calving events.

within the 250 m isobath adjacent to the Labrador Coast and some were observed offshore of Newfoundland before deteriorating below 0.25 km^2.

Ice islands originating from the 2012 calving event reached Davis Strait eight months post-calving. The ice islands, regardless if they had drifted into the deeper waters of Baffin Bay or not, again tracked to the west of the 500 m isobath once south of this location. Hudson Strait was the southernmost location that ice islands from the 2012 PG calving event were recorded, since the CI2D3 Database considered data only up to 31 December 2013.

Grounding and Bathymetry

There were 107 recorded groundings of PIIs along the east coasts of Ellesmere, Devon, and Baffin Islands and Labrador after the 2010 and 2012 Petermann calving events (Fig. 4). Grounding density is shown in Figure 4b and c. Groundings were concentrated east of Coburg Island and along the east coast of Baffin Island, specifically north of Cumberland Peninsula near the Hamlet of Qikiqtarjuaq, Nunavut. It is also noted that an ice island grounded in Navy Board Inlet, between Bylot and Baffin Islands (Fig. 4).

Several ice islands grounded in close vicinity to Coburg Island, northeast of Devon Island, where the seafloor rises to less than the 100 m depth in both the IBCAO and ETOPO1 datasets. Towards the southern extent of the drift range, three groundings associated with the 2010 calving event were recorded at the north end of the Strait of Belle Isle. In the northern reaches of the ice island drift range, ice islands associated with the 2012 PG calving event grounded in Kane Basin.

Using Ice Islands to Improve Gridded Bathymetry Products

The recorded ice island groundings occurred over bathymetry that ranged from 11 to 595 m below sea level, according to the IBCAO product. Table 1 reports the 20 locations in the ETOPO1 product where ice islands were grounded and K_d was shallower than B_{shall}. For these cases, the apparent clearance between K_d and B_{shall} ranges from 1.2 to 122.0 m. Twenty locations were flagged when assessing the IBCAO product, 15 of which were also flagged in the assessment of the ETOPO1 product. The apparent clearances for the IBCAO assessment range from 0.1 to 160.1 m. There is spatial overlap between some of the flagged grounding locations; this overlap occurs for grounding events with the following identifiers included in Table 1: KDI and XUN, ZKK and YGU, plus KYV and BOR.

Locations with potentially inaccurate bathymetry were flagged in Jones Sound, in Nares Strait east of Coburg Island, and along the east coast of central Baffin Island. Many of these locations were found in the vicinity of steep slopes (e.g., Jones Sound). Most (89%) of the potentially inaccurate B_{shall} values flagged in the IBCAO product were interpolated values (i.e., TID 41), which we consider to be unreliable (Table 1). Two of the 19 B_{shall} values, VVZ and HMZ, were associated with reliable measurements (i.e., TID 70, from pre-generated grids; Table 1). Of the seven repeat observations in the VVZ grounding, 89% to 100 % of the IBCAO grid cells under the ice island polygons were from reliable data. For the polygons that correspond with the nine repeat observations at the HMZ grounding, only 47% to 72% of the grid cells were derived from reliable data.

At locations flagged in the evaluation of the ETOPO1 product, the apparent clearance was reduced with the IBCAO evaluation in 14 cases (Table 1, down arrows), increased in 6 cases (up arrows), and was unchanged (± 5 m, double-headed arrow) in four cases. Of these, five reductions in clearance were enough to un-flag the grounding locations in the IBCAO evaluation (grounding event identifiers: LOC, LZV, NIZ, TYF, ZSD). Four locations that were not flagged in the ETOPO1 evaluation were flagged with positive apparent clearances in the IBCAO evaluation (grounding event identifiers: FGA, KDI,

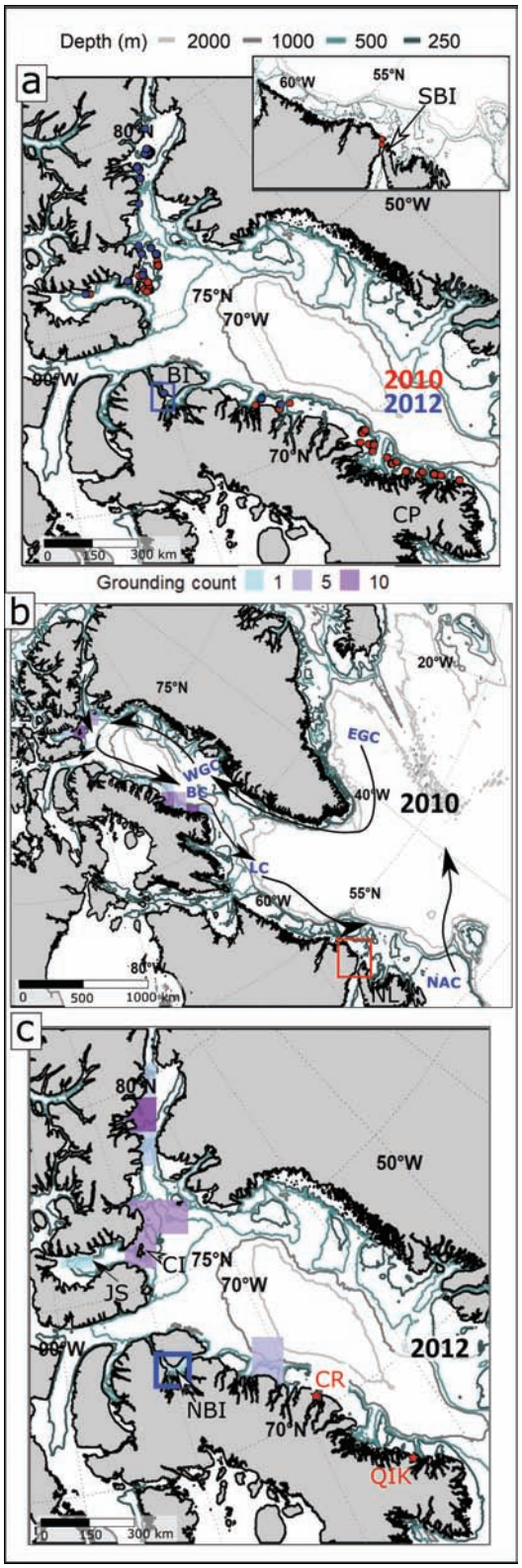

FIG. 4. Grounding locations after the 2010 and 2012 PG calving events. Panels show the individual groundings (a) and the density of groundings per 100 × 100 km grid cell following the (b) 2010 and (c) 2012 Petermann Glacier calving events. Locations of interest and major currents: (a) BI = Bylot Island, CP = Cumberland Peninsula, SBI = Strait of Belle Isle; b) EGC = East Greenland Current, WGC = West Greenland Current, BC = Baffin Current, LC = Labrador Current, NAC = North Atlantic Current; NL = Newfoundland and Labrador; (c) CI = Coburg Island, JS = Jones Sound, NBI = Navy Board Inlet, CR = Hamlet of Clyde River, QIK = Hamlet of Qikiqtarjuaq.

XUN, and YGU), although none of these changes were associated with reliable data types (Table 1).

DISCUSSION

The drift and fracture of the three largest and most recent calving events from the PG caused a pulse of ice island fragments through eastern Canadian waters over the following years, while ongoing melt resulted in an input of freshwater over the ice islands' drift trajectories (Crawford et al., 2018b). The ice islands originating from the 2008, 2010, and 2012 PG calving events followed the same general drift trajectory as those previously reported from northern Greenland ice shelves and floating ice tongues (Higgins, 1989; Newell, 1993; Peterson et al., 2009), and icebergs originating from other glaciers in the north and west sectors of Greenland (Hansen and Hartmann, 1998; Andersson et al., 2018; Marson et al., 2018), though many ice islands were observed to drift into adjacent passages as well. Common deviations from the nominal trajectory were observed into the steeply sided Jones and Lancaster Sounds. Similar deviations of simulated iceberg trajectories were also reported by Marson et al. (2018), and Newell (1993) noted drift into Lancaster Sound on his general maps of iceberg and ice island trajectories. These common meanders are driven by the strong intrusion of the Baffin Current into Lancaster Sound from the north (Fissel et al., 1982; Tang et al., 2004). The PIIs tracked in the CI2D3 Database generally did not drift deeper than the 500 m isobath within Lancaster Sound, though ice islands occasionally reached shallower waters in western Lancaster Sound as well as Navy Board and Admiralty Inlets, potentially being influenced by a secondary, southwestwardly surface current at the mouth of Lancaster Sound and variable currents north of Borden Peninsula (Fissel et al., 1982).

PII drift south of Lancaster Sound is largely directed by the Baffin Current, which is strongest along the steep continental slope of Baffin Island (Fig. 2; Fissel et al., 1982; Tang et al., 2004). The PIIs that deviated from this track and reached the deep waters in central Baffin Bay were of the smallest size classes (0.25 – 1 km^2, 1 – 10 km^2). It is hypothesized here that these smaller ice islands are more susceptible to rerouting from wind forcing than larger ice islands with greater mass that have greater momentum to overcome and are subject to greater pressure gradient and Coriolis forcing (Crocker et al., 2013). Tang et al. (2004) also described a discrepancy in drift trajectory based on iceberg size in western Greenland waters, and Marson et al. (2018) highlighted the influence of geostrophic current on the simulated drift of thick (250 m) icebergs. A full analysis of the response to environmental forcing given ice island size requires an assessment of drift trajectories and environmental conditions over the full lifespan of each ice island. While this larger assessment and comparison to non-tabular icebergs is outside the scope of this study, the CI2D3 Database would be valuable for such an investigation.

TABLE 1. Summary of locations with bathymetry flagged as potentially inaccurate. These are related to groundings where a series of ice island polygons had a conservatively estimated maximum ice draft (K_d) above the shallowest underlying pixel (B_{shall}) leading to a positive apparent clearance value. The shallowest pixel underlying all of the ice island polygons associated with a single grounding is reported in the B_{shall} column. Locations not flagged in one of the two gridded products are denoted by a short dash. The changes in apparent clearance when comparing IBCAO to ETOPO1 are grouped into five categories denoted by arrow symbols and colour coded by data type associated with the IBCAO B_{shall} data.

	GROUNDING			ETOPO1			IBCAO v4			ETOPO1 to IBCAO
Identifier	K_d (m)	Latitude (° N)	Longitude (° W)	Number of flagged polygons	B_{shall} (m)	Apparent clearance (m)	Number of flagged polygons	B_{shall} (m)	Apparent clearance (m)	Clearance change[1]
BOR	−120.8	69.227	65.61	8	−149	28.2	4	−124.6	3.8	↓
FGA	−255.0	77.041	77.536	–	–	–	12	−264.1	9.1	↑↑
HMZ	−120.8	76.329	76.215	9	−223	102.2	9	−131.1	10.4	↓
JEA	−255.0	76.164	85.111	7	−467	212.0	7	−353.6	98.7	↓
KDI	−120.8	76.247	78.48	–	–	–	13	−120.9	0.2	↑↑
KYV	−120.8	69.208	65.633	22	−187	66.2	22	−146.1	25.3	↓
LOC	−120.8	69.643	65.665	30	−155	34.2	–	–	–	↓↓
LZV	−120.8	76.453	76.162	4	−128	7.2	–	–	–	↓↓
MBF	−120.8	75.767	78.457	12	−188	67.2	12	−188.9	68.2	↕
MLZ	−120.8	76.003	77.981	7	−142	21.2	7	−144.5	23.7	↕
NIZ	−120.8	71.34	70.048	11	−159	38.2	–	–	–	↓↓
NLJ	−120.8	76.861	76.221	11	−156	35.2	10	−120.9	0.1	↓
QON	−120.8	69.162	65.631	1	−216	95.2	1	−226.9	106.1	↑
QQZ	−120.8	75.812	78.079	41	−167	46.2	41	−149.9	29.2	↓
RGW	−120.8	76.433	76.158	8	−146	25.2	4	−121.8	1.1	↓
TYF	−120.8	69.616	65.812	150	−122	1.2	–	–	–	↓↓
TYT	−120.8	76.095	78.214	3	−131	10.2	3	−135.6	14.8	↕
VIN	−120.8	75.858	78.624	4	−158	37.2	4	−133.1	12.3	↓
VVZ	−120.8	76.358	76.25	7	−198	77.2	7	−130.9	10.1	↓
XUN	−120.8	76.245	78.479	–	–	–	1	−121.5	0.7	↑↑
YBD	−120.8	76.082	78.145	3	−153	32.2	3	−148.6	27.8	↕
YGU	−120.8	75.92	78.014	–	–	–	14	−130.6	9.8	↑↑
ZKK	−120.8	75.915	78.025	3	−123	2.2	12	−131.1	10.3	↑
ZSD	−120.8	68.427	64.869	19	−322	201.2	–	–	–	↓↓

[1] ↑↑ Increased apparent clearance and new location flag; ↑ increased apparent clearance; ↕ change in apparent clearance within ± 5 m; ↓ decrease in apparent clearance; ↓↓ decrease in apparent clearance and location flag is removed. Blue arrows indicate that the data type associated the IBCAO B_{shall} value is reliable (i.e., measured directly [TID 10–17] or from a pre-generated grid [TID 70], provided by NCEI and NONNA-100 and including multibeam soundings from the CCGS *Amundsen* up to 2013). Orange arrows indicate that the data type associated with the IBCAO B_{shall} value is unreliable (i.e., interpolated or predicted data [TID 40–41]).

Figure 2 shows ice islands again tracked to the west while passing Davis Strait, which is characterised by a strong current directed to the southwest (Tang et al., 2004). PIIs that made it to these southerly waters tracked close to the east coast of Labrador and Newfoundland while directed by the Labrador Current (Newell, 1993). Almost all observations of ice islands in this vicinity were within the 0–250 m isobath. At the time that PIIs were observed in these southerly waters, one year after the 2010 PG calving event, ice islands were spread over a latitudinal span of ~30°. PIIs at the northern reaches of the drift region were thwarted by relatively shallow waters in Kane Basin in which numerous groundings occurred. Groundings were also common east of Devon Island, southeast of the Hamlet of Clyde River and off the north coast of the Cumberland Peninsula near the Hamlet of Qikiqtarjuaq. The decay of the grounded ice islands at the latter location results in a high meltwater input in this vicinity (Crawford et al., 2018b), and smaller fragments produced through ice island fracture are known to drift into the adjoining fjords of southern Baffin Island (J. Moesesie, pers. comm. 2016). In 2018 the collision of an iceberg with the seafloor in Southwind Fjord triggered a submarine landslide, demonstrating that iceberg grounding presents a geohazard with a larger footprint than the iceberg itself (Normandeau et al., 2021).

Fragments that drifted into the fjords of southern Baffin Island fell below the size-tracking threshold of the CI2D3 Database. Such icebergs and small ice island fragments are recognized as risks to natural resource extraction operations, such as those on the shallow Grand Banks of Newfoundland (Crocker, 1993; Newell, 1993; Savage et al., 2000; Peterson, 2005). The CI2D3 Database provides an opportunity to extend the assessment of ice island hazard occurrence (e.g., C-CORE, 2005; McGonigal et al., 2011) to the eastern Canadian Arctic and sub-Arctic, though further analysis is also required to assess the production and drift of smaller ice hazards in this region.

The CI2D3 Database also presented an opportunity to develop an approach for flagging potentially inaccurate seafloor heights in gridded/interpolated bathymetry products. Twenty-four of the 107 ice island groundings

assessed in this study were located over bathymetry too deep for grounding to occur given a conservative estimate of ice island keel depth (K_d). Many of these were located near Coburg Island and the southeast coast of Ellesmere Island. One location was flagged in Jones Sound and a few near the Hamlet of Qikiqtarjuaq on the east coast of Baffin Island. These flagged locations are obviously constrained to where ice islands drift, and the bathymetry issues there may not be important for navigational purposes. Nonetheless, this approach underscores the need for more accurate hydrographic surveys in Nunavut waters. We therefore recommend that these locations be properly surveyed when feasible.

The apparent clearance at each of these locations gives an approximate indication of how much the bathymetry may be in error. For example, for the IBCAO product evaluation, some of the apparent clearances are up to 100 m (Table 1; QON and JEA), suggesting that the bathymetry at these locations is 100 m too deep, whereas some apparent clearances are ~1 m or less. These apparent clearances are just enough to surpass the flagging threshold (Table 1; identifiers NLJ, RGW, and XUN). In contrast, the ETOPO1 clearances range up to 212 m, which belies the quality of this data set. This may be directly related to the accuracy of the bathymetry, the product's lower horizontal resolution, or both. The lower apparent clearance in ETOPO1 versus the IBCAO v4 dataset was expected, given the greater amount of directly observed data incorporated into the IBCAO v4 product in comparison to the ETOPO1 product. It is important to note that the apparent clearance is a relative measure that depends on the validity of the estimated ice island draft, which is the parameter K_d in this approach.

Our approach for evaluating gridded bathymetry products can tune the parameter K_d to alter the test sensitivity. Users may wish to modify K_d to be more or less conservative depending on their purpose. A K_d that is more conservative (deeper) will identify fewer locations that have potentially inaccurate bathymetry with greater certainty, whereas a less conservative (shallower) K_d will flag more locations, but may be prone to false positives. For example, we ran our script with K_d values derived from the maximum thickness values from the sections of Petermann Glacier that calved in 2010 and 2012 and returned 29 flagged locations (containing a total of 312 polygons) using IBCAO bathymetry. Another run using the maximum ice thickness plus 50% resulted in 11 flagged locations (114 individual polygons).

Altering K_d also changes the number of flagged locations associated with reliable data. For example, five locations associated with reliable B_{shall} values were flagged using the K_d derived from maximum ice thickness. This number dropped to two locations with our nominal thickness plus 25% derivation of K_d. Our evaluation yielded only one flagged location with a reliable B_{shall} for thickness plus 50%.

The greater the certainty in the ice island keel depth estimate and its corresponding maximum value (K_d), the more valid our approach becomes. Future work may improve our method by experimenting with various ways of measuring or estimating K_d. K_d could be calculated from measurements of ice island thickness or draft derived from altimetry (Bouhier et al., 2018), ice penetrating radar (Crawford et al., 2020), active seismic (Halliday et al. 2012) or acoustic methods (e.g., as used by the Canadian Arctic Through-flow project; H. Mellings, pers. comm. 2017, Crawford et al., 2018b). If these samples are representative, a theoretical maximum could be calculated by adding a specified number of standard deviations to this mean value. There is also the possibility of using bathymetric data itself to calibrate the K_d of ice islands. In this case, the K_d of an ice island (lower bound) can be verified if it drifts over shallow regions where the bathymetry is very reliably surveyed. Lastly, it may also be possible to constrain ice island keel depth estimates by accounting for thinning over time with a modelling approach (Crawford et al., 2018b). This procedure, however, introduces further assumptions and uncertainty, so we opted to test our conceptual framework using the ice thickness at calving, with the understanding that it would thin on its journey south by some unquantified amount.

Our method can detect where bathymetric data may be inaccurate because of a bias too deep. Another possible extension of our conceptual framework, albeit a more challenging one, is the possibility of flagging locations that may be reported as too shallow. To do this, ice islands with a known keel depth must be observed to drift over areas where, according to the bathymetry, they should be grounded.

An end user of this approach will need to individually consider locations that are associated with reliable B_{shall} values on a case-by-case basis. It will be necessary to determine if the potential for interpolation error exists because direct measurements are sparse in the vicinity or if the flag should be removed given the data type and thoroughness of direct measurements. The underlying data type reflected in each IBCAO grid cell is helpful to interpret where interpolation and other errors may be located. In our assessment, the majority of the grid cells that were flagged as potentially inaccurate were derived from indirect methods (e.g., interpolation). There were also grid cells flagged as inaccurate that were derived from pre-generated grids from ship sonar among other observational data sources (TID = 70 in the unknown group of data types). This finding was confirmed when the IBCAO data at these grounding positions were compared with the Canadian Hydrographic Service's NONNA-100 digital product and the U.S. National Centers for Environmental Information (NCEI) Multibeam Mosaic. The bathymetry at these locations aligned closely between the three products, which is not surprising since IBCAO v4 is derived, in part, from NONNA-100 and CCGS *Amundsen* data acquired up to 2013.

Our IBCAO results indicate that groundings VVZ and HMZ were flagged in spite of having a B_{shall} derived from what we consider to be reliable pre-generated grid data

(TID 70). In the case of HMZ, our review of individual ice island polygons indicated that 47% to 73% of the underlying pixels were of this data type at two ends of the polygons with a swath of interpolated data in between (i.e., the middle third, lengthwise, of the ice island). We surmise that the true B_{shall} is in this region and that the interpolation algorithm had insufficient data to predict a rise in the seafloor at this location. Our examination of the VVZ location indicated that these ice island polygons were underlain by a near complete or complete coverage of pre-generated grid data. We are not able to explain why B_{shall} was less than K_d at this site. It is possible that our K_d might have been too shallow by ~10 m (the apparent clearance at this location).

We evaluated our approach to flag inaccurate bathymetric data using an older, lower resolution dataset (ETOPO1) against a newer higher resolution one that incorporates more observations (IBCAO v4). We demonstrate that our approach works successfully given that apparent clearances were reduced in 14 of the 20 flagged ETOPO1 locations. Five of these locations had high enough B_{shall} values to un-flag the bathymetric data. There were some cases where clearances increased from ETOPO1 to IBCAO, however, in all six of these cases this occurred in regions where the IBCAO bathymetry was interpolated, not directly measured. While this is not ideal, it remains consistent with our expectations and does not invalidate our approach.

CONCLUSION

This work contributes a descriptive assessment of ice island occurrence in relation to regional bathymetry following calving events at the Petermann Glacier over the years 2008–12. The synthesis can be used by regulators (e.g., the Nunavut Impact Review Board, National Energy Board, Transport Canada) that need to be aware of the distribution patterns and potential drift locations of these potential ice hazards when reviewing policy or project proposals that concern the regional marine environment. Through an examination of the CI2D3 Database, it is apparent that a general pattern of ice island drift along the steep bathymetry that tracks continental shelf boundaries holds, and there is a greater probability of occurrence in these regions. Grounding is observed over the full range over which these ice islands drifted, with particularly high grounding densities observed in Kane Basin, east of Coburg Island, and along the southeast coast of Baffin Island. Combining ice island drift and grounding with better estimates of ice island keel depths may reveal as yet uncharted shoals. Such an assessment would contribute to efforts to combine disparate data sources to develop improved bathymetry products of the Arctic, including the GEBCO, IBCAO and AtaaMap: the Canadian Arctic BedMap (https://sites.google.com/ualberta.ca/ataamap) by constraining seafloor heights where data is otherwise lacking. Direct measurements of bathymetry in the Canadian Arctic are sparse (Chénier et al., 2018) and use of nontraditional data sources, such as crowd-sourced seafloor heights and satellite-derived grounding locations, will be required in this and other remote regions to achieve the goal of global bathymetric coverage (e.g., Seabed 2030 Project, https://seabed2030.org). Such efforts to constrain seafloor height are critical for marine navigation (Chénier et al., 2018) and oceanographic research. We contribute one approach to evaluating gridded bathymetry products with observations of ice island grounding and knowledge of ice island thickness. Users of this approach could use the K_d values to constrain seafloor heights in extensively interpolated, gridded bathymetry products.

This evaluation of ice island occurrence was made possible with the comprehensive CI2D3 Database. The open access CI2D3 Database also provides a unique opportunity to assess ice island drift and deterioration (Crawford et al., 2018a; Zeinali-Torbati et al., 2021), validate operational models, develop remote sensing identification and tracking techniques, and refine bathymetry products. Updated versions of the database, which will include records of ice islands originating from ice shelves fringing northern Ellesmere Island, are planned for future release through the Polar Data Catalogue (record number 12678). In regard to the next anticipated calving event of the Petermann Glacier ice tongue, researchers associated with the Water and Ice Research Lab at Carleton University (Ottawa, Canada) are ready to monitor the drift of this ice island with Cryologger tracking beacons (https://cryologger.org/tracking/) currently installed in situ.

ACKNOWLEDGEMENTS

We would like to thank all team members associated with the Canadian Ice Island Drift, Deterioration and Detection (CI2D3) Database project, which received funding and support through Environment and Climate Change Canada (ECCC), Polar Knowledge Canada, the Canada Foundation for Innovation, the Ontario Research Fund, and the Canadian Ice Service (ECCC). We also appreciate input from Luc Desjardins regarding the CI2D3 Database creation, Andrew Hamilton (University of Alberta) and Gabriel Joyal regarding bathymetric products, Adam Garbo regarding Cryologger deployments, and Andreas Münchow (University of Delaware) regarding the thickness of the 2010 and 2012 Petermann ice islands. Scripts used to analyse the bathymetric products are available at https://github.com/wirl-ice/ice-islands-and-bathymetry-products.

REFERENCES

Andersson, L.E., Scibilia, F., Copland, L., and Imsland, L. 2018. Comparison of statistical iceberg forecast models. Cold Regions Science and Technology 155:69–89. https://doi.org/10.1016/j.coldregions.2018.07.003

Amante, C., and Eakins, B.W. 2009. ETOPO1 1 Arc-minute global relief model: Procedures, data sources and analysis. NOAA Technical Memorandum NESDIS NGDC-24. Boulder, Colorado: National Geophysical Data Center, NOAA. https://doi.org/10.7289/V5C8276M

Bouhier, N., Tournadre, J., Rémy, F., and Gourves-Cousin, R. 2018. Melting and fragmentation laws from the evolution of two large Southern Ocean icebergs estimated from satellite data. The Cryosphere 12(7):2267–2285. https://doi.org/10.5194/tc-12-2267-2018

C-CORE. 2005. Characterization of ice-free season for offshore Newfoundland. C-Core Report R-04-091-341, Version 2. St. John's, NL: C-CORE and Ian Jordaan and Associates. https://www.cnlopb.ca/wp-content/uploads/news/ccorereportaddendum.pdf

Chénier, R., Faucher, M.-A., and Ahola, R. 2018. Satellite-derived bathymetry for improving Canadian Hydrographic service charts. ISPRS International Journal of Geo-Information 7(8): 306. https://doi.org/10.3390/ijgi7080306

Crawford, A.J., Crocker, G., Mueller, D., Desjardins, L., Saper, R., and Carrieres, T. 2018a. The Canadian Ice Island Drift, Deterioration and Detection (CI2D3) Database. Journal of Glaciology 64(245):517–521. https://doi.org/10.1017/jog.2018.36

Crawford, A.J., Mueller, D., Desjardins, L., and Myers, P.G. 2018b. The aftermath of Petermann Glacier calving events (2008–2012): Ice island size distributions and meltwater dispersal. Journal of Geophysical Research: Oceans 123(12):8812–8827. https://doi.org/10.1029/2018JC014388

Crawford, A.J., Mueller, D., Crocker, G., Mingo, L., Desjardins, L., Dumont, D., and Babin, M. 2020. Ice island thinning: Rates and model calibration with in situ observations from Baffin Bay, Nunavut. The Cryosphere 14(3):1067–1081. https://doi.org/10.5194/tc-14-1067-2020

Croasdale, K., Brown, R., Campbell, P., Crocker, G., Jordaan, I., King, T., McKenna, R., and Myers, R. 2001. Iceberg risk to seabed installations on the Grand Banks. Proceedings of the 16 International Conference on Port and Ocean Engineering under Arctic Conditions, 12–17 August 2001, Ottawa, Ontario. 1019–1028. https://nrc-publications.canada.ca/eng/view/accepted/?id=9babcf35-63d4-4372-ad1e-49d926b6392b

Crocker, G.B. 1993. Size distributions of bergy bits and growlers calved from deteriorating icebergs. Cold Regions Science and Technology 22(1):113–119. https://doi.org/10.1016/0165-232X(93)90050-I

Crocker, G., Carrieres, T., and Tran, H. 2013. Ice island drift and deterioration forecasting in eastern Canada. Proceedings of the 22nd International Conference on Port and Ocean Engineering under Arctic Conditions, 9–12 June 2013, Espoo, Finland. 1215–1224.

Desjardins, L., Crawford, A., Mueller, D., Saper, R., Schaad, C., Stewart-Jones, E., and Shepherd, J. 2018. Canadian Ice Island Drift, Deterioration and Detection database (CI2D3 Database), version 1.1. Waterloo, Ontario: Canadian Cryospheric Information Network. https://www.polardata.ca/pdcsearch/?doi_id=12678

Dowdeswell, J.A., and Bamber, J.L. 2007. Keel depths of modern Antarctic icebergs and implications for sea-floor scouring in the geological record. Marine Geology 243(1-4):120–131. https://doi.org/10.1016/j.margeo.2007.04.008

Dowdeswell, J.A., and Jeffries, M.O. 2017. Arctic ice shelves: An introduction. In: Copland, L., and Mueller, D., eds. Arctic ice shelves and ice islands. Dordrecht: Springer Netherlands. 3 – 21. https://doi.org/10.1007/978-94-024-1101-0_1

Fissel, D.B., Lemon, D.D., and Birch, J.R. 1982. Major features of the summer near-surface circulation of western Baffin Bay, 1978 and 1979. Arctic 35(1):180–200. https://doi.org/10.14430/arctic2318

Fuglem, M., and Jordaan, I. 2017. Risk analysis and hazards of ice islands. In: Copland, L., and Mueller, D., eds. Arctic ice shelves and ice islands. Dordrecht: Springer. 395–415. https://doi.org/10.1007/978-94-024-1101-0_15

Gille, S.T., Metzger, E.J., and Tokmakian, R. 2004. Seafloor topography and ocean circulation. Oceanography 17(1):47–54. https://doi.org/10.5670/oceanog.2004.66

Halliday, E., King, T., Bobby, P., Copland, L., and Mueller, D. 2012. Petermann Ice Island "A" survey results, offshore Labrador. The Offshore Technology Conference, 30 April–3 May 2012, Houston, Texas. OTC-23714-MS. https://doi.org/10.4043/23714-MS

Han, G., Lu, Z., Wang, Z., Helbig, J., Chen, N., and de Young, B. 2008. Seasonal variability of the Labrador Current and shelf circulation off Newfoundland. Journal of Geophysical Research: Oceans 113(C10): C10013. https://doi.org/10.1029/2007JC004376

Hansen, K.Q., and Hartmann, H. 1998. Berg Watch 97: Iceberg drift data and satellite imagery in eastern Baffin Bay. Technical Report 97-10. Copenhagen: Danish Meteorological Institute.

Higgins, A.K. 1989. North Greenland ice islands. Polar Record 25(154):207–212. https://doi.org/10.1017/S0032247400010809

Hill, B.T. 2006. Ship collision with iceberg database. Proceedings of the SNAME 7th International Conference and Exhibition on Performance of Ships and Structures in Ice, 16–19 July 2006, Banff, Alberta. https://doi.org/10.5957/ICETECH-2006-117

Hill, E.A., Carr, J.R., and Stokes, C.R. 2017. A review of recent changes in major marine-terminating outlet glaciers in northern Greenland. Frontiers in Earth Science 4: 111. https://doi.org/10.3389/feart.2016.00111

Jakobsson, M., Mayer, L.A., Bringensparr, C., Castro, C.F., Mohammad, R., Johnson, P., Ketter, T., et al. 2020. The International Bathymetric Chart of the Arctic Ocean, Version 4.0. Scientific Data 7: 176. https://doi.org/10.1038/s41597-020-0520-9

Luckman, A., Padman, L., and Jansen, D. 2010. Persistent iceberg groundings in the western Weddell Sea, Antarctica. Remote Sensing of Environment 114(2):385–391. https://doi.org/10.1016/j.rse.2009.09.009

Marson, J.M., Myers, P.G., Hu, X., and Le Sommer, J. 2018. Using vertically integrated ocean fields to characterize Greenland icebergs' distribution and lifetime. Geophysical Research Letters 45(9):4208–4217. https://doi.org/10.1029/2018GL077676

McGonigal, D., Hagen, D., and Guzman, L. 2011. Extreme ice features distribution in the Canadian Arctic. 21st International Conference on Port and Ocean Engineering under Arctic Conditions, 11–14 July 2011, Montreal, Québec. 677–686.

Meier, W.N., Hovelsrud, G.K., Van Oort, B.E.H., Key, J.R., Kovacs, K.M., Michel, C., Haas, C., et al. 2014. Arctic sea ice in transformation: A review of recent observed changes and impacts on biology and human activity. Reviews of Geophysics 52(3):185–217. https://doi.org/10.1002/2013RG000431

Merino, N., Le Sommer, J., Durand, G., Jourdain, N.C., Madec, G., Mathiot, P., and Tournadre, J. 2016. Antarctic icebergs melt over the Southern Ocean: Climatology and impact on sea ice. Ocean Modelling 104:99–110. https://doi.org/10.1016/j.ocemod.2016.05.001

Mueller, D.R., Crawford, A., Copland, L., and Van Wychen, W. 2013. Ice island and iceberg fluxes from Canadian High Arctic sources. Final draft report prepared for the Innovation Policy Group, Transport Canada. https://doi.org/10.22215/wirl/2023.2.22

Münchow, A., Padman, L., and Fricker, H.A. 2014. Interannual changes of the floating ice shelf of Petermann Gletscher, North Greenland, from 2000 to 2012. Journal of Glaciology 60(221):489–499. https://doi.org/10.3189/2014JoG13J135

Newell, J.P. 1993. Exceptionally large icebergs and ice islands in eastern Canadian waters: A review of sightings from 1900 to present. Arctic 46(3):205–211. https://doi.org/10.14430/arctic1345

NIRB (Nunavut Impact Review Board). 2019. Strategic environmental assessment in Baffin Bay & Davis Strait, Vol. 2: Background information. NIRB File No. 17SN034. Cambridge Bay: NIRB.

NOAA National Geophysical Data Center. 2009. ETOPO1 1 arc-minute global relief model. Boulder, Colorado: NOAA National Centers for Environmental Information. https://doi.org/10.7289/V5C8276M

Normandeau, A., MacKillop, K., Macquarrie, M., Richards, C., Bourgault, D., Campbell, D.C., Maselli, V., Philibert, G., and Clarke, J.H. 2021. Submarine landslides triggered by iceberg collision with the seafloor. Nature Geoscience 14:599–605. https://doi.org/10.1038/s41561-021-00767-4

Peterson, I.K. 2005. Large tabular icebergs and ice islands off eastern Canada in 2001–2003 and their probable source. Proceedings of the 18th International Conference on Port and Ocean Engineering Under Arctic Conditions, 26–30 June 2005, Potsdam, New York. 143–152.

———. 2011. Ice island occurrence on the Canadian east coast. Proceedings of the 21st International Conference on Port and Ocean Engineering under Arctic Conditions, 11–14 July 2011, Montreal, Québec. 687–696.

Peterson, I.K., Prinsenberg, S.J., Pittman, M., and Desjardins, L. 2009. The drift of an exceptionally-large ice island from the Petermann Glacier in 2008. Proceedings of the 20th International Conference on Port and Ocean Engineering under Arctic Conditions, 9–12 June 2009, Luleå, Sweden. 1047–1056.

Savage, S.B., Crocker, G.B., Sayed, M., and Carrieres, T. 2000. Size distributions of small ice pieces calved from icebergs. Cold Regions Science and Technology 31(2):163–172. https://doi.org/10.1016/S0165-232X(00)00010-0

Smith, K.L., Jr., Sherman, A.D., Shaw, T.J., and Sprintall, J. 2013. Icebergs as unique Lagrangian ecosystems in polar seas. Annual Review of Marine Science 5(1):269–287. https://doi.org/10.1146/annurev-marine-121211-172317

Smith, L.C., and Stephenson, S.R. 2013. New Trans-Arctic shipping routes navigable by midcentury. Proceedings of the National Academy of Sciences 110(13):E1191–E1195. https://doi.org/10.1073/pnas.1214212110

Stern, A.A., Johnson, E., Holland, D.M., Wagner, T.J.W., Wadhams, P., Bates, R., Abrahamsen, E.P., et al. 2015. Wind-driven upwelling around grounded tabular icebergs. Journal of Geophysical Research: Oceans 120(8):5820–5835. https://doi.org/10.1002/2015JC010805

Tang, C.C.L., Ross, C.K., Yao, T., Petrie, B., DeTracey, B.M., and Dunlap, E. 2004. The circulation, water masses and sea-ice of Baffin Bay. Progress in Oceanography 63(4):183–228. https://doi.org/10.1016/j.pocean.2004.09.005

Viehoff, T., and Li, A. 1995. Iceberg observations and estimation of submarine ridges in the western Weddell Sea. International Journal of Remote Sensing 16(17):3391–3408. https://doi.org/10.1080/01431169508954636

Wickham, H., Chang, W., Henry, L., Pedersen, T.L., Takahashi, K., Wilke, C., Woo, K., Yutani, H., and Dunnington, D. 2020. ggplot2: Create elegant data visualisations using the grammar of graphics. https://ggplot2.tidyverse.org/reference/ggplot2-package.html#author

Zeinali-Torbati, R., Turnbull, I.D., Taylor, R.S., and Mueller, D. 2021. A probabilistic model for fracture events of Petermann ice islands under the influence of atmospheric and oceanic conditions. The Cryosphere 15(12):5601–5621. https://doi.org/10.5194/tc-15-5601-2021